Electron correlation in metal clusters, quantum dots and quantum rings

2009 J. Phys. A: Math. Theor. 42 214019

(http://iopscience.iop.org/1751-8121/42/21/214019)

IOP PUBLISHING JOURNAL OF PHYSICS A: MATHEMATICAL AND THEORETICAL

J. Phys. A: Math. Theor. **42** (2009) 214019 (13pp) doi:10.1088/1751-8113/42/21/214019

Electron correlation in metal clusters, quantum dots and quantum rings

M Manninen[1] **and S M Reimann**[2]

[1] Nanoscience Center, Department of Physics, University of Jyväskylä, FIN-40014, Finland
[2] Mathematical Physics, Lund Institute of Technology, SE-22100 Lund, Sweden

Received 30 September 2008, in final form 3 December 2008
Published 8 May 2009
Online at stacks.iop.org/JPhysA/42/214019

Abstract

This paper presents a few case studies of finite electron systems for which strong correlations play a dominant role. In simple metal clusters, the valence electrons determine the stability and shape of the clusters. The ionic skeleton of alkali metals is soft, and cluster geometries are often solely determined by electron correlations. In quantum dots and rings, the electrons may be confined by an external electrostatic potential formed by a gated heterostructure. In the low-density limit, the electrons may form the so-called Wigner molecules, for which the many-body quantum spectra reveal the classical vibration modes. High rotational states increase the tendency for the electrons to localize. At low angular momenta, the electrons may form a quantum Hall liquid with vortices. In this case, the vortices act as quasi-particles with long-range effective interactions that localize in a vortex molecule, in much analogy with the electron localization at strong rotation.

PACS numbers: 73.21.La, 73.22.−f, 74.25.Qt, 73.20.Jc

(Some figures in this article are in colour only in the electronic version)

1. Introduction

For a long time, the homogeneous electron gas has been the standard theoretical model for a correlated, infinite Coulombic system where the fermionic character of the electrons plays a dominant role [1]. The so-called jellium model of a metal has been a starting point for developing functionals for the density functional theory of electrons [2]. The long-range nature of the Coulomb interaction has posed a challenge to many-body theory over many decades. At high densities of the electron gas the exchange interaction dominates, while in the low-density limit the electrons may form a Wigner crystal [3].

In real metals, the ions do not form an homogeneous charge background as in the simple jellium model, but may rather be described by a lattice of pseudo-potentials. Nevertheless, many properties of alkali metals can be understood on the basis of the jellium model, as

for example, the surface energy and work function [4], the vacancy formation energy [5], or collective plasmon excitations [1], etc. Since this works well for the bulk, it is not surprising that the jellium model also applies well to the approximate description of the properties of small alkali metal clusters [6, 7].

The intention of this paper is to provide a brief survey of some of the fascinating properties of clusters or quantum dots. In section 2, we discuss metal clusters on the basis of a two-component plasma and show that the overall shape and the plasmon excitations can be qualitatively explained by this simple model. In semiconductor heterostructures, the valence electrons may be confined in a quasi two-dimensional layer, forming a two-dimensional electron gas (2DEG). Here, depending on the material parameters, the electron density is small and the electron wavelength is much larger than the lattice constant. Consequently, the model of the two-dimensional homogeneous electron gas is valid, if the electron mass is replaced by an effective mass determined by the band structure, and the Coulomb interaction is replaced by an interaction screened by the dielectric constant of the semiconductor [8]. With etching techniques and external gates, electrons can be localized in a nearly harmonic confinement. In section 3, we will study the fascinating many-particle physics of this seemingly simple system: one example of its surprisingly rich physics is the occurrence of internally broken symmetries such as spin density waves in the ground state.

Sections 4 and 5 concentrate on the localization of electrons confined in quantum rings or 2D quantum dots. We will see how the reduction of the dimensionality increases the electron–electron correlation and how the Pauli exclusion principle then comes to play the dominating role. Using a simple model for a quantum ring, we show in section 4 that the many-particle energy spectrum reveals the internal structure of the ground state, and its analysis provides information about the Wigner localization. The collective excitations of the particles are then the classical vibrational modes of the Wigner molecule. Correspondingly, in section 5 we then show how all the low-energy states at high angular momenta can be described by a simple model Hamiltonian of a vibrating molecule. In section 6, we turn to a discussion of collective excitations at low angular momenta. For large numbers of electrons, the low-energy excitations correspond to vortices in the quantum system. The localization of vortices in a 'vortex molecule' then determines the fine structure of the energy spectrum. We connect the discussion to the physics of other, but intimately related many-body systems, such as for example cold atoms in traps, pointing out the apparent similarities between finite fermionic or bosonic quantum systems.

2. Metal clusters as electron–ion plasma

Mie [9] has shown already, 100 years ago, that a metal sphere has an optical absorption at a frequency which is independent of the size of the sphere. The absorption peak corresponds to a surface plasmon related to the bulk plasmon as $\omega_{\rm sp} = \omega_{\rm p}/\sqrt{3}$. Since the simplest model for a metal cluster is a conducting sphere, it is apparent that similar plasmon peaks as to those predicted by Mie were observed in [10]. As mentioned above, the jellium model assumes the ions to be distributed in a homogenous, rigid charge background. Modeling the cluster as a jellium sphere, the conduction electrons are then confided in the cluster by the Coulomb attraction of the sphere [11–13]. The confining potential inside the sphere is harmonic, meaning that the center-of-mass motion of the electron cloud can be separated from the internal motion. The collective oscillation of the electrons against the background charge is the plasmon of the metal sphere. This result, in fact, emerged also from a shell–model type of calculation for the correlated electrons in the cluster [14]. The phenomenon is analogous to the giant resonance in nuclei, where the protons oscillate against the neutrons [15]. A more

detailed calculation shows that the electrons spill out slightly from the region of the harmonic well. This causes a small redshift of the plasmon peak (for a review, see [7]). Experiments with large spherical alkali-metal clusters have shown that the plasmon peak occurs in fair agreement with this simple model [10].

The spherical jellium model predicted a shell structure for small sodium clusters which was observed first by Knight *et al* [16]. Immediately after this discovery, however, it was realized that only metal clusters with a filled electron shell are nearly spherical, while others should have strong (quadrupole) deformations, in much analogy with the physics of atomic nuclei [17]. Below, we shall discuss the origin of this shape deformation by considering the sodium metal as a two-component plasma consisting of ions and electrons [18]. The ions are mimicked by positrons (but shall not allow annihilation with electrons). A cluster of such a fictive 'electron–positron' plasma can be studied using the density functional Kohn–Sham method, with the single-particle equations

$$-\frac{\hbar^2}{2m}\nabla^2\psi_i + v_{\text{eff}}\psi_i = \epsilon\psi_i, \qquad v_{\text{eff}}(\mathbf{r}) = \frac{\delta V[n]}{\delta n(\mathbf{r})}, \tag{1}$$

where the effective potential is the functional derivative of the potential energy functional $V[n]$, as indicated. In the case of our imaginary electron–positron system, the potential energy consists only of the exchange and correlation energies since the total Coulomb potential (Hartree term) is zero due to the symmetry (the electron and positron densities are identical). Alternatively, we can imagine the positive ions forming a completely deformable, 'floppy' (classical) background charge which will always take the same density distribution as the electron density, but does not have its own correlation or exchange energy. This is the so-called ultimate jellium model [19] where the potential energy is now *only* the exchange and correlation energy of the electron gas, $V[n] = E_{\text{xc}}[n]$. The equilibrium density of the infinite ultimate jellium is close to that of the electron density of sodium (with a Wigner–Seitz parameter of $r_s \approx 4.2a_0$, where a_0 is the Bohr radius). Nevertheless, it is still surprising how well the model can quantitatively describe shape-related properties of real sodium clusters [20]. The obtained shapes are in agreement with those determined by the splitting of the plasmon resonance into two separate peaks [21].

The success of the simple plasma model for describing the overall shapes of sodium clusters is based, on the one hand, on the softness of the metal, and on the other hand, on the universality of the shapes of small fermion systems [22]. In small systems, there are only a small number of single-particle states which contribute to the density distribution. The effective potential is a functional of this density distribution and will thus have a similar shape determined by a few single-particle wavefunctions, irrespective of the details of the interparticle interactions binding the system together. In fact, Häkkinen *et al* [22] have shown that the cluster *shape* (but not size) is remarkably insensitive to the specific form of the potential functional, $V[n]$ in equation (1), leading to 'universal' shapes and explaining why even the functional for the nuclear matter produces the same shapes as obtained for jellium clusters [23]. Consequently, the two above-mentioned models, the electron–positron plasma and the ultimate jellium model, give the same shapes, but different particle densities.

As an example, figure 1 illustrates the strength of this universality, showing the results for three *a priori* very different models for clusters containing 6 and 14 particles. The density contours of the two clusters on the left are the results of the universal model (or the so-called ultimate jellium model) where the only essential parameter is the average density of the bulk material. The cluster shapes shown in the center panel are the results of *ab initio* density functional calculations using *ab initio* pseudo-potentials. The right panel shows the results of the simplest possible tight-binding model, which assumes constant bond length and only

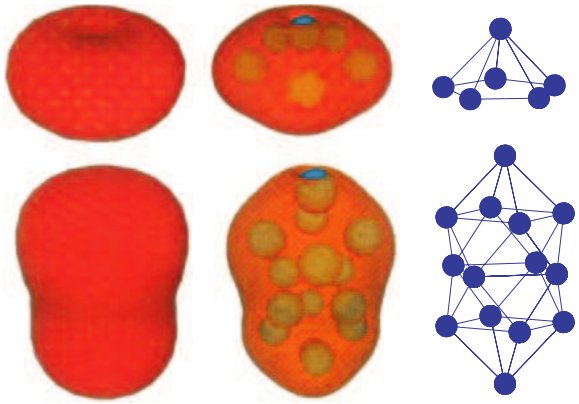

Figure 1. Shapes of clusters with 6 and 14 particles. The left panel shows the constant-density surface of the universal model giving similar shapes irrespective of the interparticle interactions. The center panel shows the constant-density surface and ion positions in sodium clusters calculated within DFT. The right panel shows stick-and-ball models of atom positions of TB clusters. Note that in this case the constant-density surface cannot be defined, but the resulting atom positions are the same as in the DFT calculation.

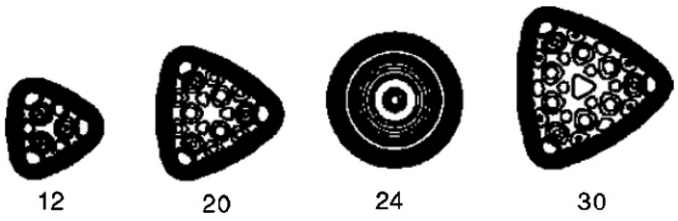

Figure 2. Electron densities in 2D plasma clusters calculated with the ultimate jellium model. Note that the sizes 12, 20 and 30 correspond to filled shells.

nearest neighbor hopping. Note that this tight-binding model does not take into account any long-range Coulomb interactions.

The above analysis only explains the generic features of photoabsorption and shapes of metal clusters. *Ab initio* electronic structure calculations have been used to study the detailed atom positions as well as photoabsorption and photoemission spectra [20, 24–29]. These calculations have reached an accuracy that, combined with experiments, they can reliably reveal the atomic structure of small metal clusters. In the case of sodium clusters the electronic shell structure has been observed at temperatures where the clusters are in a liquid state [30]. Computational work has confirmed that the shell structure resists the melting transition [31].

In semiconductors, it is possible to make two-dimensional structures where electrons and holes are at different layers, the separation of the layers hindering their recombination. In the limit of the vanishing interlayer distance the electrons and holes form a two-dimensional plasma. Reimann *et al* [40] studied finite-size systems of such a 2D plasma and observed that, like in 3D, the shapes of the plasma clusters are quite robust. Interestingly, in 2D those clusters corresponding to filled electronic shells of 2D circular traps do not have circular shapes but strong triangular deformations, as shown in figure 2. The reason is that in a triangular cavity the lowest-energy shells agree with those of the harmonic oscillator [41].

It has also been suggested [42, 43] that the two-dimensional deformable jellium model could capture the main correlations of alkali metal clusters on a weakly interacting substrate, like oxide or graphite. In such systems computations based on DFT and pseudo-potentials [22] indeed also result in a triangular shape for $N = 12$ in agreement with the simple model.

3. Two-dimensional quantum dots: DFT

In the previous sections, we studied free metal and plasma clusters and learned that, just like in nuclei, any open-shell system is deformed with respect to the spherical shape. In 2D, even closed-shell clusters do not necessarily occur only for circular shape. The internal symmetry breaking is driven by the tendency to maximize the energy gap between the highest occupied and the lowest unoccupied single-particle state, in accordance with the Jahn–Teller theorem. In the remaining parts of this brief survey, let us consider the systems where the electrons (or ions and atoms, respectively) are trapped by a rigid harmonic confinement. Physical examples of such systems are the conduction electrons in semiconductor quantum dots, as well as atoms and ions confined in magneto-optical traps.

Generally speaking, with interactions between the particles, the degeneracy of an open shell can be reduced by spin polarization driven by Hund's first rule. However, this mechanism may compete with other, internal, symmetry breakings (for reviews see [32, 33]). Examples are deformation effects (as discussed above for metal clusters and the jellium model), pairing (like in nuclei for interactions with an effectively attractive part) or the formation of a spin density wave (see below).

Tunneling spectroscopy of small quantum dots [45] has clearly revealed the energy-lowering of the half-filled shells due to Hund's first rule. The results are strongly supported by the spin-density functional [46] and *ab initio* many-particle calculations for electrons in a harmonic confinement (for a review see [8]).

In the low-density electron gas, the electrons localize in a Wigner crystal. Close to this limit, the difference of the total energy between the paramagnetic and the ferromagnetic electron gas diminishes. When the electrons localize, the spin ordering is expected to follow the Heisenberg model for the spin. Density functional theory in the local density approximation cannot describe properly the Wigner crystal, since the Coulomb self-interaction of the localized electrons is not properly canceled by the local exchange. In order to study particle localization, despite an *a priori* lack of correlation, it was argued that it is then more favorable to use the unrestricted Hartree–Fock method [33, 47] or other many-particle methods, such as the configuration interaction (CI) method or the quantum Monte Carlo (for a review see [33]).

At large densities, i.e. $r_s \leqslant 6a_0^*$ (here a_0^* is the effective Bohr radius), the six-electron quantum dot has a closed-shell configuration. Its ground state is a state with total spin $S = S_z = 0$ in both the CI and SDFT methods, with circularly symmetric particle densities. As r_s increases, however, the total density remains azimuthally symmetric, while the spin densities show a symmetry breaking leading to a pronounced spatial oscillation in the spin polarization (see figure 3), but still total spin $S_z = 0$. Such so-called spin density wave (SDW)-like states [46] have been much discussed in the literature, and it was claimed that such states are simple artifacts of the broken spin symmetries in SDFT [48, 49]. To resolve this question, clearly one has to compare the SDFT results with the solutions of the full many-body Hamiltonian. The many-particle state of a few electrons in a quantum dot can be obtained numerically nearly exactly by diagonalizing the Hamiltonian in a properly restricted Hilbert space. However, density and spin densities of the exact solution necessarily have the same symmetry as the Hamiltonian. For a circular quantum dot, this means that the solutions also must have the azimuthal symmetry of the Hamiltonian. Consequently, the possible localization

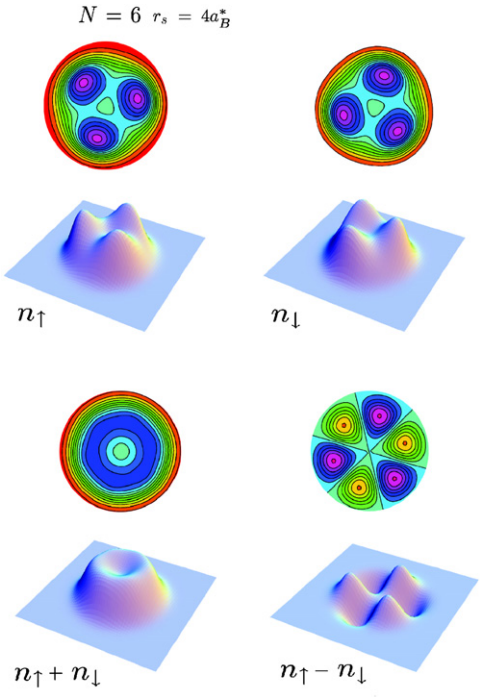

Figure 3. DFT spin densities $n^\uparrow$ and $n^\downarrow$ (upper panel) and total density ($n^\uparrow + n^\downarrow$) as well as (unnormalized) spin polarization ($n^\uparrow - n^\downarrow$) (lower panel) for a six-electron quantum dot at $r_s = 4a_0^*$, shown as 3D plots and their contours (from [56]).

of electrons, or other internal symmetry breakings such as the above-mentioned spin-density waves, can not be seen directly in the total particle- or spin-densities. Instead, one then has to investigate the pair-correlation functions, i.e., conditional probabilities, to study the internal structure [52, 53]. Indeed, the direct comparison to spin-dependent pair-correlation functions in the configuration interaction method clearly demonstrated that SDW-like states in question can appear in the internal structure of the exact many-body state [56]. However, the SDFT results remain questionable for the discussion of spin multiplets, as already shown by von Barth in 1979 [50].

In a multi-component system, the particles may have also other internal degrees of freedom than the spin. These can be, for example, electrons in different layers of a semiconductor heterostructure or electrons corresponding to different conduction electron minima in a multi-valley semiconductor. For many internal degrees of freedom, the DFT–LDA can capture even the localization of particles in the low-density limit [51].

In the frequently applied Monte Carlo method (see [54] for a review) the electron localization can be mapped by following the electron paths, a finite number of Monte Carlo steps [55]. It should be mentioned that Monte Carlo methods have also been used to study the shell structure in quantum dots [34, 35]. In an external magnetic field a two-dimensional quantum dot is a finite-size realization of a quantum Hall liquid. In this case, trial wavefunctions can be used to study the internal structure of the quantum state [36, 37] (for a review see [38]). An elegant trial wavefunction for a rotating system in the Wigner molecule limit has also been presented [39].

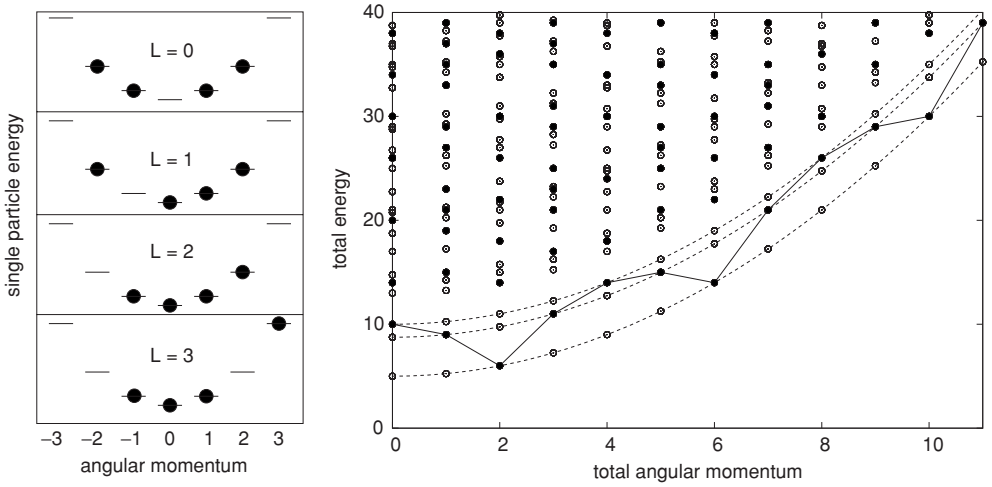

Figure 4. Spectra of one-dimensional quantum rings. The right panel shows the spectrum of four particles interacting with a delta function interaction in a strictly 1D ring. Black bullets show results of the states with maximum spin ($S = 2$), circles have lower spin. The solid line connects the lowest states of polarized electrons. The dashed lines show the (lowest) rigidly rotating state and the lowest vibrational states. The left panel shows the configurations of the lowest-energy states of polarized electrons for $L = 0, \ldots, 3$, demonstrating how the lowest-energy state is obtained for $L = 2$.

In the rest of this paper, we will focus on the many-body energy spectrum and show that in some cases it can be directly used as a signature of particle localization. We will first consider the simple case of a one-dimensional quantum ring.

4. Energy spectra and localization: quantum rings

In a strictly one-dimensional ring, the single-particle energy levels are solutions to the angular momentum part of the Hamiltonian,

$$H = -\frac{\hbar^2}{2mR^2}\frac{\partial^2}{\partial\phi^2}, \tag{2}$$

where R is the radius of the ring. The solutions are $\psi_\ell(\phi) = \exp(\mathrm{i}\ell\phi)$ with energy eigenvalues $\epsilon_\ell = \hbar^2\ell^2/2mR^2$. For simplicity, we will consider non-interacting electrons with the same spin. Then each electron occupies a different single-particle state, and the energy is the sum of the energies of the single-particle energies. Figure 4 shows, as an example, the resulting (here non-interacting) many-particle energy spectrum for four (spinless) electrons.

More generally, we can consider particles interacting with an infinitely strong contact interaction ($v(\mathbf{r}-\mathbf{r}') = v_o\delta(\mathbf{r}-\mathbf{r}')$, where $v_0 \to \infty$). Note that for polarized electrons, the contact interaction then does not play any role since the Pauli exclusion principle forbids the electrons to be at the same point. The many-particle problem (with spin) for contact interactions can be solved exactly with the Bethe ansatz [57, 58].

Figure 4 shows that for non-polarized electrons, the lowest energy of each angular momentum (the so-called yrast state) is a smooth function of L, while for polarized electrons it oscillates with a period of four. The reason for this oscillation becomes obvious when one considers the configurations of each of these states, as illustrated in the figure. If there is

a non-occupied state between the occupied ones, the energy is higher than for the compact states. The period of four is a result of the following fact: if Ψ_L is a solution for a ring of N particles with the angular momentum L then also

$$\Psi_{L+\nu N} = \exp\left(\mathrm{i}\nu \sum_k^N \phi_k\right) \Psi_L \tag{3}$$

is a solution with the angular momentum $L + \nu N$. Moreover, both of these states have exactly the same internal structure. One can interpret the eigenenergies in figure 4 as a rotation–vibration spectrum of localized electrons. The states at the minima (the lowest dashed line) correspond to rigid rotations of localized electrons while the states above have vibrational states accompanying the rigid rotation (two lowest vibrational states are shown as dashed lines). The possibility of vibrational states of non-interacting electrons is a peculiarity of the 1D system: an electron is localized between the two neighboring electrons since the Pauli exclusion principle prevents them from passing each other. This gives an effective $1/r^2$ interaction between the electrons which in this case arises from the kinetic energy of the electrons. Indeed, quantizing the vibrational models of a ring formed of particles with $1/r^2$ interactions gives exactly the spectrum shown in figure 4.

In quasi-one-dimensional rings with electrons interacting by long-range Coulomb interactions, the localization may also be seen directly in the energy spectrum. If the electrons are non-polarized, the charge and spin degrees of freedom separate. The charge excitations are the rigid rotations and vibrations, while the spin excitations can be described by the anti-ferromagnetic Heisenberg model of localized spins [59] (for a review see [58]). The conclusion is that in narrow quantum rings the electrons localize in a 'necklace' of electrons and the collective low-energy excitations are vibrations and spin excitations.

5. Rotation–vibration spectrum of electrons in quantum dots

Let us now return to electrons confined in a 2D harmonic potential and consider first the rotational states of polarized electrons with large angular momentum. The electrons interact by their long-range Coulomb interaction. For not too large numbers of electrons, the Hamiltonian can be solved numerically almost exactly. Maksym [60, 61] showed that the resulting energy spectrum can be quantitatively described by quantizing the classical vibrational modes solved in a rotating frame. Figure 5 shows that for high angular momenta the whole energy spectrum can be quantitatively described by the vibration modes of the localized particles.

Figure 5 shows that the lowest-energy state as a function of the angular momentum has a similar periodicity of four as observed above for four electrons in a ring. The figure also shows pair-correlation functions for three cases. For $L = 54$, the pair-correlation function shows that the electrons are clearly localized: fixing the position of one reference electron fixes the positions of the three other electrons. In the cases $L = 56$ and $L = 57$, the localization does not seem to be as strong due to the fact that these states correspond to vibrational excitations (for a more detailed analysis, see [62]).

Let us consider the effects of the electron spin on the many-particle spectrum and on the electron localization. Note that the Hamiltonian of the system does not depend on spin (since there is no magnetic field or spin–orbit interaction). However, as already noted in connection with the discussion of particles on a ring, the spin-degree of freedom has an important role in making the total wavefunction antisymmetric. Moreover, it turns out that in the case of a long-range Coulomb interaction, the localized electrons interact with an effective exchange interaction as in the Heisenberg anti-ferromagnet. In the case of a one-dimensional ring, this

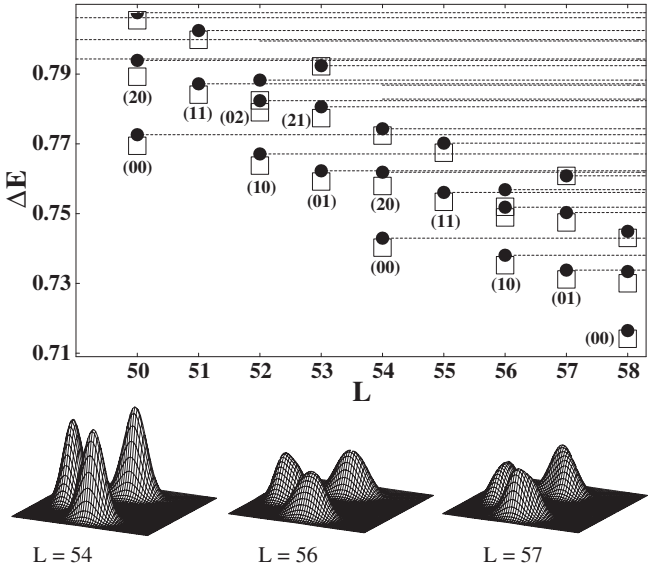

Figure 5. Energy spectrum of four polarized electrons in a 2D quantum dot. The black bullets show the result of an exact quantum-mechanical diagonalization calculation, while the circles are results of the quantization of the vibrations and rotations of classical electrons of a Wigner molecule. The numbers (nm) show the occupancies of the two vibrational modes of the system. The lower panel shows the pair-correlation functions of the lowest-energy states for three angular momenta. The energy is in atomic units and $\Delta E = E_i - L\hbar\omega_0$, where $\omega_0 = 1$ is the confinement frequency.

can be understood on the basis of the half-filled Hubbard model with the nearest neighbor hopping [58, 66]. The effective Hamiltonian for electrons localized in a ring can be written as

$$H_{\text{eff}} = \frac{\hbar^2}{2I}\mathbf{M}^2 + \sum_{\nu} \hbar\omega_\nu n_\nu + J \sum_{\langle i,j \rangle} \mathbf{S}_i \cdot \mathbf{S}_j, \tag{4}$$

where I is the moment of inertia, ω_ν is the eigenfrequency of the vibrational mode ν, J is an effective exchange interaction and S_i is the spin operator. The value of J becomes smaller when the localization gets more pronounced. In the case of the infinitely strong contact interaction discussed in the previous section, $J = 0$ and the spin-excitations have zero energy. For Coulomb interactions J is always finite leading to finite spin excitations.

Figure 6 illustrates the effect of the spin in the cases of a 2D dot and a quasi-1D ring with four electrons. In both cases, the lowest band corresponds to a rigid rotation of the electrons localized in a square. An energy gap separates these states from the vibrational excitations. In both cases, the low-energy spectrum is similar and consistent with the model Hamiltonian. The antisymmetry requirement dictates which spin–state is allowed at the given angular momentum. Group theory can be used to resolve the allowed states. We note that the low-energy state for the maximum spin ($S = 2$) appears at the angular momentum 2, in accordance with the simple model for quantum rings shown in figure 4. The energy differences between the different spin states in the ring are consistent with the Heisenberg Hamiltonian (the last term in equation (4)). For the dot, the order of the spin states for angular momentum 4 is different, most likely due to the fact that in this case there is also an exchange interaction between the opposite corners of the square of the four electrons, omitted in the simple model.

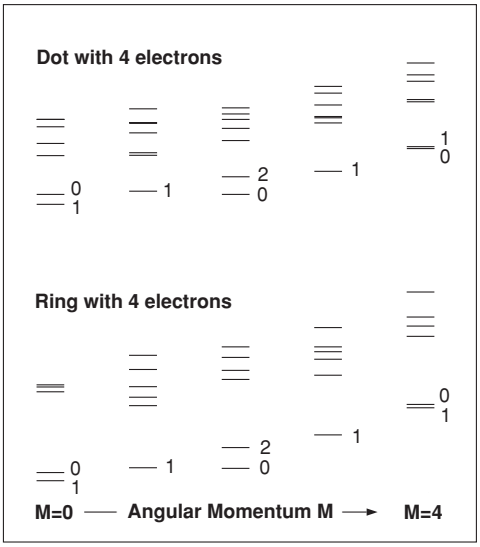

Figure 6. Many-particle energy spectrum for four electrons in a 2D quantum dot and in a quantum ring. The numbers next to the lowest-energy levels show the total spin of the state.

6. Localization of vortices and energy spectrum

In the previous section, we showed that the electron localization in a quantum dot shows characteristic features in the rotational spectrum. Especially, in the case of a few particles the geometry of the localized molecule, i.e. the symmetry group, determines the periodic features of the spectrum as a function of the angular momentum. The same method can be used to study localization of vortices in 2D quantum dots. A strong magnetic field will polarize the 2D electron gas in the quantum dot and put it in a rotational state. At the angular momentum $L = N(N-1)/2$, the rotating electrons form a quantum Hall liquid (QHL) with the filling factor 1. In the case of a quantum dot, this state is usually called the 'maximum density droplet' (MDD) [63]. If the magnetic field is increased, the angular momentum grows and vortices form in the system. The vortices effectively have a repulsive long-range interaction between them, which causes their arrangement in a regular geometric pattern, such as has been seen experimentally in the case of superconductors [67], as well as dilute atom gases in traps [64].

Evidence for the localization of vortices is also found directly in the many-particle spectrum of polarized electrons. Figure 7 shows the low-energy spectrum of 20 electrons, calculated using the exact diagonalization technique. A smooth function of L is subtracted from the spectrum to emphasize the details of the yrast line. The figure shows that below $L \approx 210$ the yrast line is a smooth function. Beyond this value, the yrast line oscillates with a period of two, three and four. These oscillations result from the existence of two, three or four localized vortices in the system. The lowest points correspond to a rigid rotation of the ring of vortices, while the higher energies correspond to vibrational excitations of the vortex system.

If the single-particle basis is restricted to the lowest Landau level, i.e. to those single-particle states of the 2D harmonic oscillator that have no radial oscillations, we can use particle–hole duality to further analyze the localization of vortices [68]. In a polarized

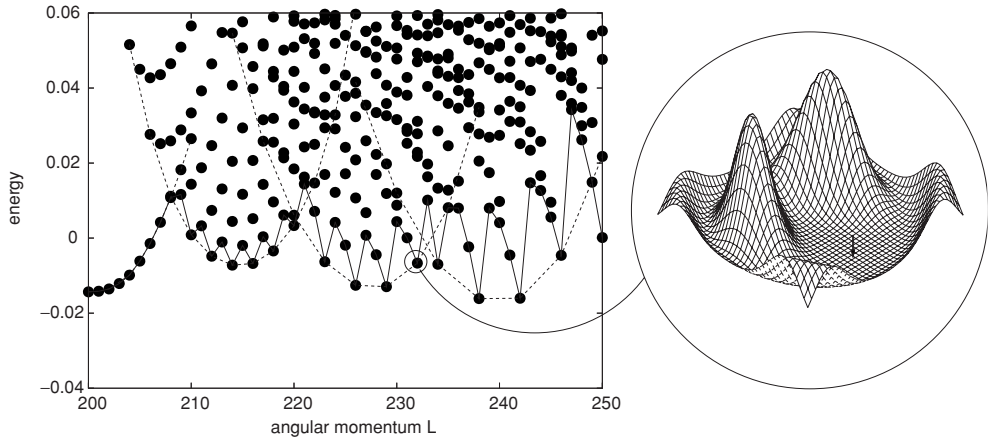

Figure 7. Energy spectrum of 20 polarized electrons in a 2D quantum dot showing the periodic oscillations arising from localization of two, three and four vortices, when the angular momentum is increased. The hole–hole pair-correlation corresponding to one of the states is shown on the right, showing the localization of the three vortices (the reference vortex is fixed at the point of the arrow).

Fermi system, we can describe any quantum state in the occupation number representation equivalently by the particles or the holes. In our present system, the holes correspond to the vortices and, consequently, the hole–hole correlation function describes the spatial correlation between the vortices. Figure 7 shows the hole–hole correlation for one of the states in the three-vortex region, showing clearly the localization of the three vortices at the corners of an equilateral triangle. Let us finally recall that most theoretical studies of vortices in quantum Hall liquids are based on the trial wavefunction approach [33, 36, 37, 65]. This approach also explains the similarity of vortex formation in fermion and boson systems [69].

7. Conclusions

This paper is *not* meant to be a comprehensive review of correlation effects in a small system of electrons. Rather, we have looked at selected case studies where the small size and low dimension of the systems emphasize the correlation and the collective motion of the electrons.

In the first section, we showed that in small clusters of simple metals it is the optimal shape of the electron cloud that dictates the overall geometry of the cluster making the ions the electrons' slaves. The electron–ion system behaves like a structureless plasma, where the electron–electron exchange and the correlation energy determine the shape of the cluster. In small systems, this correlation is so strong that, in fact, it does not matter what kind of internal interaction the particles have or what kind of physical model is used for the system, as illustrated in figure 1.

A strong external confinement hinders the spatial deformation. At low densities or high rotation, the electrons tend to localize in Wigner molecules. The energy spectrum is then dominated by the rigid rotation and the internal vibrations of the molecule. The localization also separates the spin-excitations from the vibrational charge excitations, as most clearly seen in quasi-1D rings. A model Hamiltonian consisting of rigid rotations, quantized vibrations and an anti-ferromagnetic Heisenberg model describes well the low-energy spectrum of the system. All low-energy excitations are thus collective excitations of strongly correlated electrons.

At high magnetic fields the electrons in a quantum dot form a 'miniature' quantum Hall liquid of polarized electrons. In this case, the elementary collective excitations are vortices. Interestingly, the vortices have a similar energy spectrum as the localized electrons. For example, the spectrum of three localized electrons shows the same vibrational modes as the spectrum of three vortices. The vortices can be interpreted as holes in the occupied Fermi sea, and the hole–hole correlation function can be used to confirm the localization of the vortices.

References

[1] Fetter A L and Walecka J D 1971 *Quantum Theory of Many-Particle Systems* (New York: McGraw-Hill)
[2] Kohn W and Sham L J 1965 *Phys. Rev.* **140** A1133
[3] Wigner E P 1934 *Phys. Rev.* **46** 1002
[4] Lang N D and Kohn W 1970 *Phys. Rev.* B **1** 4555
[5] Manninen M, Nieminen R, Hautojärvi P and Arponen A 1975 *Phys. Rev.* B **12** 4012
[6] de Heer W A 1993 *Rev. Mod. Phys.* **65** 611
[7] Brack M 1993 *Rev. Mod. Phys.* **65** 677
[8] Reimann S M and Manninen M 2002 *Rev. Mod. Phys.* **74** 1283
[9] Mie G 1908 *Ann. Phys. (Leipzig)* **25** 377
[10] Bréchignac C, Cahuzac Ph, Kebaïli N, Leygnier J and Sarfati A 1992 *Phys. Rev. Lett.* **68** 3916
[11] Martins J L, Car R and Buttet J 1981 *Surf. Sci.* **106** 265
[12] Hintermann A and Manninen M 1983 *Phys. Rev.* B **27** 7262
[13] Ekardt W 1984 *Phys. Rev.* B **29** 1558
[14] Koskinen M, Manninen M and Lipas P O 1994 *Z. Phys.* D **31** 125
[15] Bohr Å and Mottelson B R 1975 *Nuclear Structure* (London: Benjamin)
[16] Knight W D, Clemenger K, de Heer W A, Saunders W A, Chou M Y and Cohen M L 1984 *Phys. Rev. Lett.* **52** 2141
[17] Clemenger K 1985 *Phys. Rev.* B **32** 1359
[18] Manninen M 1986 *Phys. Rev.* B **34** 6886
[19] Koskinen M, Lipas P O and Manninen M 1995 *Z. Phys.* D **35** 285
[20] Moseler M, Huber B, Hakkinen H, Landman U, Wrigge G, Hoffmann M A and von Issendorff B 2003 *Phys. Rev.* B **68** 165413
[21] Borggreen J, Chowdhury P, Kebaïli N, Lundsberg-Nielsen L, Lützenkirchen K, Nielsen M B, Pedersen J and Rasmussen H D 1993 *Phys. Rev.* B **48** 17507
[22] Häkkinen H, Kolehmainen J, Koskinen M, Lipas P O and Manninen M 1997 *Phys. Rev. Lett.* **78** 1034
[23] Koskinen M, Lipas P O and Manninen M 1995 *Nucl. Phys.* A **591** 421
[24] Bonačić-Koutecký V, Fantucci P and Koutecký J 1991 *Chem. Rev.* **91** 1035
[25] Kostko O, Huber B, Moseler M and von Ossendorf B 2007 *Phys. Rev. Lett.* **98** 043401
[26] Jackson K, Ma L, Yang M and Jellinek J 2008 *J. Chem. Phys.* **129** 144309
[27] Akola J, Manninen M, Häkkinen H, Landman U, Li X and Wang L-S 1999 *Phys. Rev.* B **60** R11297
[28] Kümmel S, Brack M and Reinhard P-G 2000 *Phys. Rev.* B **62** 7602
[29] Häkkinen H 2008 *Chem. Soc. Rev.* **37** 1847
[30] Bjørnholm S and Borggreen J 1999 *Phil. Mag.* B **79** 1321
[31] Rytkönen A, Häkkinen H and Manninen M 1998 *Phys. Rev. Lett.* **80** 3940
[32] Yannouleas C and Landman U 2006 *Proc. Natl. Acad. Sci. USA* **103** 10600
[33] Yannouleas C and Landman U 2007 *Rep. Prog. Phys.* **70** 2067
[34] Reusch B and Egger R 2003 *Europhys. Lett.* **64** 84
[35] Weiss S and Egger R 2005 *Phys. Rev.* B **72** 245301
[36] Laughlin R B 1983 *Phys. Rev.* B **27** 3383
[37] Jain J K 1989 *Phys. Rev. Lett.* **63** 199
[38] Viefers S 2008 *J. Phys.: Condens. Matter* **20** 123202
[39] Yannouleas C and Landman U 2003 *Phys. Rev.* B **68** 035326
[40] Reimann S M, Koskinen M, Helgesson J, Lindelof P E and Manninen M 1998 *Phys. Rev.* B **58** 8111
[41] Reimann S M, Koskinen M, Häkkinen H, Lindelof P E and Manninen M 1997 *Phys. Rev.* B **56** 12147
[42] Kohl C, Montag B and Reinhard P-G 1996 *Z. Phys.* D **38** 81
[43] Kolehmainen J, Häkkinen H and Manninen M 1997 Metal clusters on an inert surface: a simple model *Z. Phys.* D **40** 306
[44] Häkkinen H and Manninen M 1996 *J. Chem. Phys.* **105** 10565

[45] Tarucha S, Austing D G, Honda T, van der Haage R J and Kouwenhoven L 1996 *Phys. Rev. Lett.* **77** 3613
[46] Koskinen M, Manninen M and Reiman S M 1997 *Phys. Rev. Lett.* **79** 1389
[47] Yannouleas C and Landman U 1999 *Phys. Rev. Lett.* **82** 5325
[48] Hirose K and Wingren N S 1999 *Phys. Rev.* B **59** 4604
[49] Harju A, Räsänen E, Saarikoski H, Puska M J, Nieminen R M and Niemelä K 2004 *Phys. Rev.* B **69** 153101
[50] von Barth U 1979 *Phys. Rev.* A **20** 1693
[51] Kärkkäinen K, Koskinen M, Reimann S M and Manninen M 2004 *Phys. Rev.* B **70** 195310
[52] Reimann S M, Koskinen M and Manninen M 2000 *Phys. Rev.* B **62** 8108
[53] Yannouleas C and Landman U 2004 *Phys. Rev.* B **70** 235319
[54] Harju A 2005 *J. Low Temp. Phys.* **140** 181
[55] Filinov A V, Bonitz M and Lozovik Yu E 2001 *Phys. Rev. Lett.* **86** 3851
[56] Borgh M, Toreblad M, Koskinen M, Manninen M, Åberg S and Reimann S M 2005 *Int. J. Quantum Chem.* **105** 817
[57] Lieb E H and Wu F Y 1968 *Phys. Rev. Lett.* **20** 1445
[58] Viefers S, Koskinen P, Deo P S and Manninen M 2004 *Physica* E **21** 1
[59] Koskinen M, Manninen M, Mottelson B and Reimann S M 2001 *Phys. Rev.* B **63** 205323
[60] Maksym P A 1996 *Phys. Rev.* B **53** 10871
[61] Maksym P A, Imamura H, Mallon G P and Aoki A 2000 *J. Phys.: Condens. Matter* **12** R299
[62] Nikkarila J-P and Manninen M 2007 *Solid State Commun.* **141** 209
[63] MacDonald A H, Yang S R E and Johnson M D 1993 *Aust. J. Phys.* **46** 345
[64] Madison K W, Chevy F, Wohlleben W and Dalibard J 2000 *Phys. Rev. Lett.* **84** 806
[65] Jain J K and Kamilla R K 1998 *Composite Fermions: A Unified View of the Quantum Hall Effect* ed O Heinonen (River Edge, NJ: World Scientific)
[66] Kolomeisky E B and Straley J P 1996 *Rev. Mod. Phys.* **68** 175
[67] Tinkham M 1995 *Introduction to Superconductivity* (New York: McGraw-Hill)
[68] Manninen M, Reimann S M, Koskinen M, Yu Y and Toreblad M 2005 *Phys. Rev. Lett.* **94** 106405
[69] Borgh M, Koskinen M, Christensson J, Manninen M and Reimann S M 2008 *Phys. Rev.* A **77** 033615